TRIANGULAR ELEMENTS IN PLATE BENDING - CONFORMING AND NON-CONFORMING SOLUTIONS

G.P. Bazeley*
Y.K. Cheung**
B.M. Irons***
O.C. Zienkiewicz****

For some considerable time research effort has been directed at determining suitable stiffness characteristics of triangular plate elements in bending, spurred on by the necessity of dealing with irregular boundaries, doubly curved shell problems and others. The success of the direct deflection approach in establishing these properties for rectangular elements using simple polynomials (References 1 and 2) and an initial failure of a similar approach of dealing with triangular elements (Reference 7) led to some unjustified conclusions concerning necessary convergence criteria. In particular, much has been said about the absolute need for displacement and slope conformity throughout the boundary between adjacent elements as a 'sine qua non' for convergence to correct solution. The authors suggest that another condition is in fact the only necessary one and that it is possible to achieve convergence without the rather difficult conformity requirement. This new condition is that of the displacement function being capable of representing constant curvature (strain) states throughout a finite element irrespective of its size or shape.

In dealing with the triangular plate element the authors present in the paper several alternative derivations based on various explicit types of displacement functions. In all, the new requirement of 'constant curvature' is in fact, satisfied and, in addition, all but one satisfy completely the compatibility conditions. The displacement functions use the so-called 'area coordinates' to ensure symmetry and simplicity of statement. The new formulation is applied to the solution of some typical static and dynamic plate problems.

Good convergence and accuracy is achieved by the new stiffness matrices. The results are of comparable accuracy with those attainable by the use of rectangular elements. The 'non-compatible' type of solution appears to give better accuracy than the compatible one for practical element sizes.

INTRODUCTION

Considerable interest exists in the derivation of a suitable stiffness matrix for a triangular plate element subject to bending and interconnected with other elements at the nodes formed by the apices of such a triangle. The obvious need for such a solution is (a) to allow the treatment of irregular boundaries in plate bending problems, and more importantly (b) to permit the formulation of suitable programmes for solution of arbitrary doubly curved shells.

*Section Leader, Stress Office, Rolls-Royce Ltd., Derby.
**Lecturer, Civil Engineering Department, University of Wales, Swansea.
***Staff Specialist - Stress Office, Rolls-Royce Ltd., Derby.
****Professor of Civil Engineering, Chairman School of Engineering, University of Wales, Swansea.

While in the solution of plane elasticity problems the simplest formulation arises with an element of triangular form (and indeed such elements were the basis of the first useful solutions utilizing the finite element method) this does not appear to be the case with problems of plate bending. Workable solutions for rectangular plate elements have been published repeatedly (References 1 to 6) while the only reported stiffness for a triangular element has been a failure (References 7 and 8).

The reasons for this are not at all obvious, though perhaps an intuitive difficulty may be immediately observed when polynomials in rectangular Cartesian coordinates and with selected terms (Reference 7) are used to represent displacement conditions in an arbitrarily oriented triangle.

In Reference 7 the author attributes the unsatisfactory results to the use of functions not complying with slope continuity along the sides of adjacent elements. How is one to explain the fact that this condition, not satisfied in any of the rectangular elements shape functions used in the References 1 to 6 does, apparently, lead to convergence? Perhaps the difficulties are due to another cause.

In this paper a non-conforming function will be given with some derived numerical results demonstrating an apparent convergence and good accuracy. In addition corrective terms will be established for this function which permit complete continuity to be achieved.

SOME CONVERGENCE CRITERIA

In the finite element formulation the deformation of the complete structure is expressed in terms of certain displacement components at points called the nodes. The deformation function within a particular polynomial element bounded by lines joining adjacent nodes is uniquely defined by the values of the displacements at these nodes. The so-called 'equilibrium equations' derived from the element 'stiffness matrices' are simply a statement of the minimization of the total energy of the system.

In the above formulation the strain energy contribution is evaluated by integration of the infinitesimal strain energies, expressed in terms of appropriate deformation functions, over the area of each element individually. If the deformation function leads to no singularities or infinities within an element and at the junction with other elements leads to no infinite stresses (i.e. in case of plates satisfies both displacement and normal slope continuity), then clearly with an increasing number of parameters as the subdivision gets smaller convergence to the correct energy level, i.e., to the correct answer must occur, providing:

(a) the displacement function is such that self-straining due to a rigid body motion of the element is not permitted.

(b) that the displacement function within each element is such that it can express constant 'strain' conditions.

The first condition is so obvious that it has seldom been explicitly stated, yet its violation is easily achieved with certain form of deformation functions - a pitfall into which the authors have on one occasion fallen.

The second condition (which in fact embraces the first) is more rigorous. While many functions will satisfy it when elements are infinitesimal, the selection is more limited if it is also to be satisfied when the element is of finite size - and yet clearly the trivial case of constant strain should be capable of representation whatever the size of the element subdivision.

For plate elements this constant-strain condition becomes one of constant curvature requiring that the displacement function should be capable of representing a constant curvature when the nodal displacements are compatible with this requirement.

The convergence conditions so far implied that the requirement of continuity across element boundaries prevents the development of infinite strains and stresses there. For the case of plates such a requirement presupposes that both lateral displacements and normal slopes of these are continuous or otherwise infinite curvatures would be involved.

If such discontinuities at interfaces are, however, present in the nature of the displacement functions assumed then, clearly, the true strain energy is not obtained by restricting the integration to the elements alone implied in the formulation. However it is still valid to seek the solution minimizing the total energy computed on the previous basis providing also the minimization of the discontinuities is also achieved. Possibility of such an approach was presented by Jones (Reference 9) by attempting to add to the functional, based on the general Reissner formulation (Reference 10), an integral of the discontinuity terms multiplied by suitable Lagrangean multipliers.

More simply, if the formulation of the functions is such that as the element size decreases, satisfaction of continuity conditions become more and more complete, the preceding formulation of the finite element process (even though it ignores the strain energy stored at the interface regions) must tend to the correct solution. If the 'constant strain' criterion is used in the basic derivation of the displacement functions then as the elements decrease indefinitely in size the continuity at the nodes will require a constant strain state to be reached in the limit within each element. This state of constant strain will automatically require that compatibility of the deformation exists across the interfaces.

While solutions in which displacement continuity (conformity) is satisfied at all stages gives by the well known energy theorem (Reference 11) a bound on the total strain energy of the true solution which in a non-continuous solution is not present; it is nevertheless possible for the latter type of solution to present, for practical engineering purposes, a better approximation than that given by the former.

A NONCONFORMING DEFORMATION FOR A TRIANGULAR PLATE ELEMENT

'Area' Coordinates.

The use of a polynomial in Cartesian coordinates x and y to define the shape of a triangular element with 9 degrees of freedom involves some arbitrary elimination of certain terms involved in the full cubic (which contains 10 terms) (Reference 7). For an arbitrary triangle this is 'aesthetically' not pleasing, involving as it does, the choice of certain preferential directions unrelated to the triangle shape.

To avoid this difficulty it is convenient to use so-called area coordinates specifying the position of any point P inside an arbitrary triangle 1, 2 and 3 as shown in Figure 1.

If these coordinates are called

$$L_1 = A_1/\Delta, \quad L_2 = A_3/\Delta \text{ and } L_3 = A_3/\Delta \tag{1}$$

where the total area of triangle is Δ, then it is easy to see that only two of these are independent as

$$L_1 + L_2 + L_3 = 1$$

As the area of any triangle can be defined in terms of its apex coordinates as, for instance,

$$2\Delta = \det \begin{vmatrix} 1 & x_1 & y_1 \\ 1 & x_2 & y_2 \\ 1 & x_3 & y_3 \end{vmatrix} \tag{2}$$

we can relate L_1, L_2, L_3 with the x-y coordinates as

$$\begin{aligned} L_1 &= (a_1 + b_1 x + c_1 y) / 2\Delta \\ L_2 &= (a_2 + b_2 x + c_2 y) / 2\Delta \\ L_3 &= (a_3 + b_3 x + c_3 y) / 2\Delta \end{aligned} \tag{3}$$

with

$$\begin{aligned} a_1 &= x_2 y_3 - x_3 y_2 \\ b_1 &= y_2 - y_3 = y_{23} \\ c_1 &= (x_3 - x_2) = x_{32} \end{aligned} \tag{4}$$

with others obtainable in changing suffices in cyclic order 1-2-3.

It can be noted that solving for x and y we can define alternatively

$$\begin{aligned} x &= L_1 x_1 + L_2 x_2 + L_3 x_3 \\ y &= L_1 y_1 + L_2 y_2 + L_3 y_3 \end{aligned} \tag{5}$$

Elimination of Self-Straining (Relative Displacement)

The nodal dispacements in terms of which the displacement function w is to be formulated are the three values of w and six values of the rotations of the nodal points.

For an element 1, 2 and 3, the vector with nine components defines the nodal deformations as

$$\{\delta\}^e = \begin{bmatrix} w_1 \\ \theta_{x1} \\ \theta_{y1} \\ w_2 \\ \theta_{x2} \\ \theta_{y2} \\ \omega_3 \\ \theta_{x3} \\ \theta_{y3} \end{bmatrix} \tag{6}$$

with

$$(\theta_x)_1 = \left(-\frac{\partial w}{\partial y}\right)_1 \qquad (\theta_y)_1 = \left(\frac{\partial w}{\partial x}\right)_1 \quad \text{etc.} \tag{7}$$

To eliminate the possibility of any self-stressing it is convenient to deal with displacements w^*, relative to a rigid body translation of the whole plate element with nodal displacements w_1, w_2, and w_3, which we shall denote as w^R.

Thus

$$w^* = w - w^R \tag{8}$$

and in terms of area coordinates w^R is simply given by

$$w^R = w_1 L_1 + w_2 L_2 + w_3 L_3 \tag{9}$$

which is a linear function in x and y and gives the required nodal displacements.

As w^* must have zero values at the nodes its form can be defined in terms of six slopes imposed at the nodes, $(\delta^*)^e$

$$(\delta^*)^e = \begin{bmatrix} \theta^*_{x1} \\ \theta^*_{y1} \\ \theta^*_{x2} \\ \theta^*_{y2} \\ \theta^*_{x3} \\ \theta^*_{y3} \end{bmatrix} \tag{10}$$

with

$$\theta_x^* = -\frac{\partial w^*}{\partial y} = \theta_x + \frac{\partial w^R}{\partial x} \tag{11}$$

and

$$\theta_y^* = \frac{\partial w}{\partial x} = \theta_y - \frac{\partial w^R}{\partial y} \tag{12}$$

On using Equation 9 it is easy to show that

$$\theta_{x1}^* = \theta_{x1} + (c_1 w_1 + c_2 w_2 + c_3 w_3)/2\Delta \tag{13}$$

and

$$\theta_y^* = \theta_y - (b_1 w_1 + b_2 w_2 + b_3 w_3)/2\Delta$$

Thus $(\delta)^e$ and $(\delta^*)^e$ can be related simply as

$$(\delta^*)^e = T\,(\delta)^e \tag{14}$$

in which T is a 6 x 9 transformation matrix given as

$$T = \left|\begin{array}{ccc|ccc|ccc}
\frac{c_1}{2\Delta} & 1 & 0 & \frac{c_2}{2\Delta} & 0 & 0 & \frac{c_3}{2\Delta} & 0 & 0 \\
-\frac{b_1}{2\Delta} & 0 & 1 & -\frac{b_2}{2\Delta} & 0 & 0 & -\frac{b_3}{2\Delta} & 0 & 0 \\
\hline
\frac{c_1}{2\Delta} & 0 & 0 & \frac{c_2}{2\Delta} & 1 & 0 & \frac{c_3}{2\Delta} & 0 & 0 \\
-\frac{b_1}{2\Delta} & 0 & 0 & -\frac{b_2}{2\Delta} & 0 & 1 & -\frac{b_3}{2\Delta} & 0 & 0 \\
\hline
\frac{c_1}{2\Delta} & 0 & 0 & \frac{c_2}{2\Delta} & 0 & 0 & \frac{c_3}{2\Delta} & 1 & 0 \\
-\frac{b_1}{2\Delta} & 0 & 0 & -\frac{b_2}{2\Delta} & 0 & 0 & -\frac{b_3}{2\Delta} & 0 & 1
\end{array}\right| \tag{15}$$

It is convenient to use this matrix in the numerical computations.

Polynomial Function for w^*

The function w^* has to be uniquely (and linearly) defined in terms of the six components of $(\delta^*)^e$ or

$$w^* = F_{x1}\,\theta_{x1}^* + F_{y1}\,\theta_{y1}^* + F_{x2}\,\theta_{x2}^* + F_{y2}\,\theta_{y2}^* + F_{x3}\,\theta_{x3}^* + F_{y3}\,\theta_{y3}^* \qquad (16)$$

has to be found with the 'shape functions' F being such that for instance,

$$F_{x1} = 0 = \frac{\partial F_{x1}}{\partial x} \quad \text{at all nodes}$$

$$\frac{\partial F_{x1}}{\partial y} = 0 \text{ at nodes 2 and 3}$$

$$\text{or} \quad \frac{\partial F_{x1}}{\partial y} = -1 \text{ at node 1}$$

If polynomial expressions are to be used, the simplest function which satisfies the above conditions appears to be

$$F_{x1} = y_{12}\,L_1^2\,L_2 + y_{13}\,L_1^2\,L_3$$

The verification that the appropriate conditions are satisfied is easily obtained by simple algebra.

Similarly the other functions could be obtained, e.g.

$$F_{x1} = x_{21}\,L_1^2\,L_2 + x_{31}\,L_1^2\,L_3 \text{ etc.}$$

Unfortunately it will be found that the above functions will not satisfy the 'constant curvature' conditions which is one of the basic requirements. To remedy this, the functions $L_1 L_2 L_3$ can be added in any desired proportion as this particular function gives zero slopes and deflections at all nodes. Finally, therefore, we shall write

$$F_{x1} = y_{12}(L_1^2\,L_2 + \alpha L_1 L_2 L_3) + y_{13}(L_1^2\,L_3 + \alpha L_1 L_2 L_3) \qquad (17)$$

and

$$F_{y1} = x_{21}(L_1^2\,L_2 + \alpha L_1 L_2 L_3) + x_{31}(L_1^2\,L_3 + \alpha L_1 L_2 L_3) \qquad (18)$$

with the others defined similarly.

To be able to represent any constant curvature within the element we must be able to express w^* as a simple quadratic equation

$$w^* = A_1 L_2 L_3 + A_2 L_3 L_1 + A_3 L_1 L_2 \qquad (19)$$

in which A_1, A_2, A_3 can take on any prescribed values (other quadratic terms like L_i^2 etc. are not admissible as w^* is zero at nodes). From Equation 19 it is evident that for constant curvature the nodal slopes become

$$\theta_{x1} = -(A_3 c_2 + A_2 c_2)/2\Delta = -(A_3 x_{13} + A_2 x_{21})/2\Delta$$

$$\theta_{y1} = (A_3 b_2 + A_2 b_3)/2\Delta = (A_3 y_{31} + A_2 y_{12})/2\Delta$$

On substituting into Equation 16 we have

$$2\Delta w^* = A_1(-x_{21}F_{x2} + y_{12}F_{y2} - x_{13}F_{x3} + y_{31}F_{y3})$$
$$+ A_2(-x_{32}F_{x3} + y_{23}F_{y3} - x_{21}F_{x1} + y_{12}F_{y1})$$
$$+ A_3(-x_{13}F_{x1} + y_{31}F_{y1} - x_{32}F_{x2} + y_{23}F_{y2})$$

When expressions (Equations 17 and 18) are substituted into the above it is found simply that Equation 19 can be obtained only if $\alpha = \frac{1}{2}$ and that then the constant curvature condition is possible*. Conversely also if slopes of the correct kind are imposed on Equation 16, a constant curvature solution must be obtained.

A CORRECTION FOR SLOPE CONFORMITY

The displacement functions derived for w^* (or w) vary along any side of the triangle as a cubic and as this variation is uniquely defined by the nodal values it will therefore be the same for an adjacent element and conformity of 'w' is satisfied. However the variation of the normal slope to any line is parabolic and, as a parabola is not uniquely defined by two end values, a discontinuity of slope will generally occur between elements.

It is possible to devise functions ϵ_1, ϵ_2 and ϵ_3 such that, for instance ϵ_1 has

(a) zero values along all sides of the triangle

(b) gives zero values of slopes at all nodes

(c) has zero normal slopes along sides 12 and 13

(d) has a parabolic variation of normal slope along side 23.

with ϵ_2 and ϵ_3 obeying similar conditions with respect to the other nodes.

Clearly the addition of these functions in any proportion to the original displacement function will not affect the nodal values of w or its slopes.

If the departure from linearity of the normal slope defined by Equations 16 to 19 is calculated at some typical point along each of the three sides of the element (conveniently taken as the midpoint) then, clearly, by adding suitable proportions of ϵ_1, ϵ_2 and ϵ_3 it will be possible to eliminate this and ensure a linear variation of the normal slope. This obviously will now result in continuity between adjacent elements.

---

*The coefficient of A_1 becomes

$$(L_2^2 L_3 + \alpha L_1 L_2 L_3)(x_{12}y_{23} + x_{32}y_{12})/2\Delta$$
$$+(L_3^2 L_2 + \alpha L_1 L_2 L_3)(x_{31}y_{32} + y_{31}x_{23})/2\Delta$$

and as the second term is simply the determinant 2 this gives

$$L_2 L_3 (L_2 + L_3 + 2\alpha L_1)$$

which is only equivalent to $L_2 L_3$ when $\alpha = \frac{1}{2}$.

This incidentally shows that the first expression proposed for functions F would not have satisfied the constant curvature criterion.

As the calculated departure will be a linear function of the imposed nodal rotations the corrected displacement function will not admit 'self-straining' (see Section 2). In addition, as the original function admits the constant curvature condition during which the normal slope already varies linearly, the correction term will, under such conditions, be zero. The corrected function therefore will also satisfy the 'constant strain' criterion.

At this stage it is convenient to rewrite the displacement function F as defined in Equations 17 and 18 as

$$F_{x1} = y_{12}\ \psi_{12} + y_{13}\ \psi_{13} \tag{17a}$$

$$F_{y1} = x_{21}\ \psi_{12} + x_{31}\ \psi_{13} \tag{18a}$$

in which

$$\psi_{12} = L_1^2\ L_2 + \tfrac{1}{2} L_1\ L_2\ L_3$$

with the other functions being obtained by a suitable permutation.

With the ϵ function defined in scale so as to give the maximum value of $\frac{\partial \epsilon_i}{\partial L_i}$ at midpoint of the appropriate side as $\frac{1}{4}$, it will be found that the displacement function corrected for slope conformity, w^{**} can still be defined by the same Equations 16, 17a, and 18a if

$$\psi_{12} = L_1^2\ L_2 + \tfrac{1}{2} L_1\ L_2\ L_3 - \tfrac{1}{2}\epsilon_2 + \tfrac{1}{2}\epsilon_2 + \tfrac{3}{2} K_3\ \epsilon_3\ ,\ \text{etc.} \tag{20}$$

with

$$K_3 = \frac{y_{21}(y_{23}+y_{13}) + x_{21}(x_{23}+x_{13})}{x_{12}^2 + y_{12}^2}\ ,\ \text{etc.} \tag{21}$$

The algebra involved in proving this is reasonably straightforward if lengthy and has therefore been omitted.

A possible alternative to linearizing the normal slopes is to admit the value of the normal slope (absolute not relative slope now) at some point along the side as an additional variable and retain this value in computations as an additional nodal variable. Such a formulation would follow a similar pattern utilizing the same ϵ functions, but this procedure is not desirable as it introduces additional variables and special nodes into the final formulation.

It will be noted when the various ϵ functions are considered in detail that the curvatures are not uniquely defined by them at the actual nodal points (though they do not tend to become infinite) (Reference 13). This can be shown to be a necessary corollary of the linear slope requirement and the resulting singularities cause some difficulties in the stress computation.

Three different ϵ functions will now be considered:

(i) The simplest set of corrective functions ϵ is given by

$$\epsilon_1^{(a)} = \frac{L_1 L_2^2 L_3^2}{(L_1+L_2)(L_1+L_3)} \quad \text{etc. for } c_2 \text{ and } \epsilon_3 \tag{22}$$

It is readily seen that this function has zero values at all sides and that it tends to zero at the nodes.

Similarly by differentiation it can be shown that

$$\frac{\partial \epsilon_1}{\partial x} = \frac{\partial \epsilon_1}{\partial y} = 0$$ at all nodes and along sides 12 and 13 of the triangle.

Near side 23 the Equation 22 behaves like $L_1 L_2 L_3$ and therefore has normal slopes varying parabolically as required.

(ii) The function

$$\frac{L_1^2 L_2^2 L_3^2}{(L_1+L_2)(L_2+L_3)(L_3+L_1)} \tag{23}$$

gives zero value and slopes along all sides of the triangle and therefore can be added without affecting the basic considerations.

It was thought desirable to be able even with the corrective functions present to be able to reduce the function to a cubic form. If the second form of corrective function is defined as

$$\epsilon_1^{(b)} = \epsilon_2^{(a)} + \frac{2}{3} \frac{L_1^2 L_2^2 L_3^2}{(L_1+L_2)(L_2+L_3)(L_3+L_1)} \tag{24}$$

then it can be verified that the combination:

$$\epsilon_1^{(b)} + \epsilon_2^{(b)} + \epsilon_3^{(b)} = L_1 L_2 L_3$$

and is therefore capable of reducing to an ordinary cubic.

The third possibility is that due to Clough (Reference 15). Here each of the three ϵ_1 functions is represented by three different expressions within the triangle. Dividing the triangle into three smaller triangles 1 - 2 - P, 1 - 3 - P and 2 - 3 - P where P represents the centroid of the triangle it can be shown that the function $\epsilon_1^{(c)}$ defined as below satisfies all the necessary requirements.

$$\begin{aligned}
&\text{Triangle } 2-3-P \quad \epsilon_1^{(c)} = L_1 (5L_1^2 - 3L_1 + 6L_1 L_2)/6 \\
&\text{Triangle } 1-2-P \quad \epsilon_1^{(c)} = L_2^2 (3L_3 - L_2)/6 \\
&\text{Triangle } 1-3-P \quad \epsilon_1^{(c)} = L_3^2 (3L_2 - L_3)/6
\end{aligned} \tag{25}$$

The other two functions are defined in a similar, piecewise, manner. It is easy to verify

$$\epsilon_1^{(c)} + \epsilon_2^{(c)} + \epsilon_3^{(c)} = L_1 L_2 L_3 \text{ everywhere.}$$

STIFFNESS AND STRESS MATRICES

Once the displacement functions are specified the determination of stiffness and stress matrices for elements follows the usual procedures.

In terms of relative displacement the nodal force vector consists of six couples

$$\mathbf{M}^* = \begin{bmatrix} M_{x1} \\ M_{y1} \\ M_{x2} \\ M_{y2} \\ M_{x3} \\ M_{y3} \end{bmatrix} = \mathbf{K}^* (\delta^*)^e \tag{26}$$

where $\mathbf{K}^*$ can be obtained by the usual methods (See Reference 2 or 7). The full force matrix corresponding to the absolute displacements δ^e has nine components, as given by

$$(\mathbf{F})^e = \begin{bmatrix} W_1 \\ M_{x1} \\ M_{y1} \\ \cdot \\ \cdot \\ \cdot \end{bmatrix} \tag{27}$$

As the work done by either system has to be identical

$$(\delta^*)^{e,T} \mathbf{M}^{*e} = (\delta)^{e,T} \mathbf{F}^e$$

and as this is true for any nodal displacements we have from which by use of Equations 26 and 14 that

$$\mathbf{F}^e = \mathbf{T}^T \mathbf{K}^* \mathbf{T} \delta^e \tag{28}$$

thus relating the absolute stiffness matrix to $\mathbf{K}^*$.
Similarly if the internal moments or stresses are found in the relative coordinate system

$$\sigma = \mathbf{S}^* \delta^{*e} \tag{29}$$

the use of Equation 14 gives

$$\sigma = \mathbf{S}^* \mathbf{T} \delta^e \tag{30}$$

Integration of the expressions in the stiffness matrix can be carried out in a variety of ways.

For the 'nonconforming' functions it was found most convenient to expand the shape functions or polynomials in x and y and use simple integration expressions available.

For the conforming solution explicit integrals are not simply obtainable and use was made of numerical integration techniques.

EXAMPLES OF SOLUTIONS BASED ON THE NON-CONFORMING SHAPE FUNCTION

Square, Isotropic, Plate

The relatively simple problem of a square isotropic plate under various conditions of support and loading is a convenient test example as numerous "exact" solutions are available in standard texts.

The finite element solutions were so designed that the effects of the shape of elementary triangles and the fineness of the subdivision could be studied. Figure 2 shows the six different subdivisions used in a quarter of the plate (only symmetrical cases of support and loading were considered). Five of these are based on the square module to permit direct comparison with finite difference solutions and solutions of Reference 2, but as different orientations of elementary triangles are possible here for any given size of division a variety is obtained. The last subdivision is based on an arbitrary subdivision into 16 elements which is as nearly equilateral as possible and represents a division slightly coarser than that of the (6x6) mesh.

Edges of the plate were taken alternatively as simply supported and clamped, and the loads represented either a single concentrated load P at center or a uniformly distributed load q. The allocation of the distributed load to the nodes was not done using the 'consistent load matrix' as time did not permit its integration. The 'natural' way of taking one-third of the load acting on any element and assigning this to each node was followed. Figures 3 to 5 summarized some of the results.

Figure 3 shows the deflection on the center line obtained for various meshes together with the 'exact' center values (Reference 12). In all cases excellent convergence is obtained* with even the coarsest subdivision giving results of the right order of magnitude.

Figure 4 shows the actual distribution of displacements on the finest mesh (8x8) for the clamped edge conditions. This case was studied extensively by finite difference and for comparison solutions obtained by Vaisey and Fox (Reference 13) on a 16x16 mesh are shown. It is seen that these are almost identical.

Figure 5 shows some of the bending moments computed on the center line using the finest mesh solutions. Values plotted here are the averages of nodal ones and these averages again are very close to the exact values where such have been computed. The dotted lines show the actual linear variation of moments through the element indicating the considerable nodal discontinuities, similar to those obtainable in plane stress analysis. It is interesting to note that in the solution by rectangular elements such discontinuities were much smaller (Reference 2).

Square Clamped Plate With a Circular Opening

This example for which no exact solution is available was chosen to illustrate possible application to a problem where other numerical solutions present special difficulties.

---

* Use of the central load P with simply supported condition shows the biggest divergence from the value of $560 \times 10^{-6} \frac{PL^2}{D}$ quoted by Timoshenko. This value obtained by the Ritz method is, however, approximate and slightly suspect.

The loading consists of a pair of concentrated loads P to retain symmetry conditions. Figures 6 to 9 show the results obtained.

In Figures 7 and 8 the contours of the slopes obtained by the finite element solution are shown side by side with an experimental solution by Moire methods of the same problem. The Moire fringes which again show the lines of constant slope indicate both qualitative and quantitative agreement despite the fact that in estimating the fringe constant experimental accuracy only of ±5 percent can be expected.

COMPARATIVE SOLUTIONS BASED ON CONFORMING SHAPE FUNCTIONS

Concurrently with the preceding work based on a computor program in which exact integrated expressions were used, an alternative program based on a numerical integration was written, in which the various ϵ - corrections restoring conformity could be incorporated. This programme allowed the special case of mid-side nodes to be used if desired and also the programme based on the nonconformity function could be reproduced by simply making $\epsilon = 0$. This incidentally served as one of the checks on accuracy of programming.

Numerical integration was performed by using 16 and 256 integrating points but the accuracy of the first sub-division was found to be adequate (within about 1%). Time allowed only one of the cases of section 7 to be investigated. This was the case of the square plate with uniform and central loadings. The results are summarized in Tables 1 and 2.

These results are remarkable. While the conforming types of solution converge monotonically to the correct answer underestimating the deflexions for all subdivisions, the nonconforming type of solution gives at all the stages investigated a better approximation (although the convergence in this case is not monotonic and does not give any 'bounds').

For fairly coarse subdivision the nonconforming type of solution is so much superior that some doubts existed in the authors' mind about the correctness of the various subroutines. These have, however, checked out in a variety of ways so that the chances of an error can be eliminated.

VIBRATION PROBLEMS

The new stiffness matrices were incorporated in a program by which the natural frequencies and nodal shapes of plate vibrations could be found. Such programs were described by some of the authors in a previous paper (Reference 16) in which rectangular shaped elements were used.

In the computations the mass of the plate was assigned to the nodes by a method which ensured correct amounts of virtual work being performed during any virtual motion. The derivation of such 'consistent' mass matrices is described in general terms in both References 2 and 16 and need not be repeated here.

Figure 10 shows the results of such a vibration analysis carried out for a simple, cantilever plate, for which results were available in literature (Reference 17). A very coarse division into only four triangular shaped elements was used. Once again the superiority of the answers obtained by using the nonconforming shape functions is demonstrated. These give errors in frequencies for the first four modes of the order of, -2.5, +2.5, -1.7 and +1.6 percents respectively.

With the use of the conforming solutions the best answers are obtained with the first type of corrective function. The respective errors are now +2.5, +18.0, +3.6, +33.1 percents.

As expected all frequencies are overestimated (i.e. bounds are obtained once again). The results are however, again inferior in accuracy.

The modal shapes plotted in Figure 10 are those obtained by solution $\epsilon = \epsilon^{(c)}$.

CONCLUDING REMARKS

The new function introduced into the study of triangular plate elements show that:

(a) Conforming type solutions are possible,

(b) a simple nonconforming type function is capable of giving better engineering accuracy, providing such a function satisfies the so-called 'constant strain' criterion. This was previously demonstrated on rectangular shaped elements where similar functions were used.

Methods which will ensure a further improvement in accuracy particularly with regard to stress representation, are being worked upon, but it is clear that a stage is now reached where solution to all plate and shell problems can be simply achieved.

REFERENCES

1. Adini, A., Analysis of Shell Structures by the Finite Element Method. Ph.D. Dissertation, University of California, Berkeley, Calif., 1961.

2. Zienkiewicz, O.C., and Cheung, Y.K., "The Finite Element Method for Analysis of Elastic Isotropic or Orthotropic Slabs, Proc. of the Institute of Civil Engineers, Vol. 28, p. 471, 1964.

3. Melosh, R.J., "A Stiffness Matrix for the Analysis of Thin Plates in Bending," Journal of Aeronautical Sciences, Vol. 28, p. 34, 1961.

4. Melosh, R.J., "Basis of Derivation of Matrices for the Direct Stiffness Method," AIAA Journal, Vol. 1, p. 1631, 1963.

4.(a) Tocher, J.L., and Kapur, K.K. (Comment on 4 above), AIAA Journal, Vol. 3, p. 1215, June 1965.

5. Dawe, D.J., "A Finite Element Approach to Plate Vibration Problems," Journal of Mech. Eng. Sci., Vol. 7, p. 28, 1965.

6. Goyan, R.J., "Distributed Mass Matrix for Plate Element Bending," AIAA Journal, Vol. 3, p. 567, 1965.

7. Clough, R.W., "The Finite Element in Structural Mechanics., Chapter 7, Stress Analysis, O.C. Zienkiewicz and G.S. Holister, Ed., J. Wiley and Sons, 1965.

8. Tocher, J.L., Analysis of Plate Bending Using Triangular Elements. Ph. D. Dissertation, University of California, Berkeley, Calif., 1962.

   Jones, R.E., "A Generalization of the Direct Stiffness Method of Structural Analysis," AIAA Journal, Vol. 2, No. 5, p. 821, 1964.

10. Reissner, E., "On a Variational Theorem in Elasticity," Journal of Mathematics and Physics, Vol. 29, p. 90, 1950.

11. Fraeijs de Veubeke, B., Chapter 9, loc. cit. Ref. 7.

12. Timoshenko, S., and Woinowsky-Krieger, S., Theory of Plates and Shells. McGraw-Hill Book Co., 2nd edition, 1959.

13. Irons, B. Draper, K., "Inadequacy of Nodal Connections in a Stiffness Solution for Plate Bending," AIAA Journal, Vol. 3, p. 965, 1965.

14. Southwell, R.V., Relaxation Methods in Theoretical Physics. Clarendon Press, Oxford, 1956.

15. Clough, R.W. and Tocher, J.L. A Private Communication.

16. Zienkiewicz O.C., Irons B., Nath B., Natural Frequencies of Complex, Free or Submerged Structures by the Finite Element Method. Proc. Symp. on Vibration in Civil Engineering. Inst. Civ. Eng., April, 1956.

17. Barton, M.V., Vibration of Rectangular and Skew Cantilever Plates. J. Applied Mechs Vol. 18, p. 129-134, 229, June 1951.

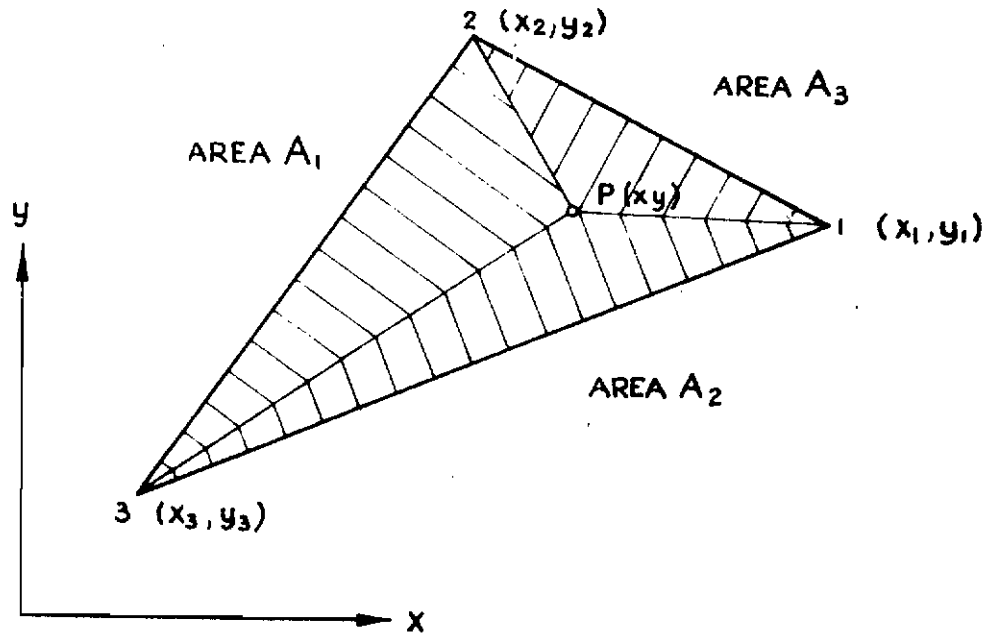

Figure 1. Area Coordinates

TABLE 1 CENTRAL LOAD ON SQUARE PLATE

Values of $Dw_{max}/10^{-5}\ PL^2$

a. Simply Supported Edges.

	$\epsilon = 0$	$\epsilon = \epsilon^{(a)}$	$\epsilon = \epsilon^{(b)}$	$\epsilon = \epsilon^{(c)}$
2 x 2 mesh	1302	855	854	798
4 x 4 mesh	1176	1057	1056	1039
6 x 6 mesh	1211	1117	1116	1108
8 x 8 mesh	1165			

Conforming solutions

Exact value 1160.

b. Clamped Edges

	$\epsilon = 0$	$\epsilon = \epsilon^{(a)}$	$\epsilon = \epsilon^{(b)}$	$\epsilon = \epsilon^{(c)}$
2 x 2	521	193	186	169
4 x 4	589	474	472	461
6 x 6	583	511	510	503
8 x 8	572			

Exact value 560.

TABLE 2 DISTRIBUTED LOAD ON A SQUARE PLATE

Values of $Dw_{max}/10^{-5}\ qL^4$

a. Simply Supported Edges

	$\epsilon = 0$	$\epsilon = \epsilon^{(a)}$	$\epsilon = \epsilon^{(b)}$	$\epsilon = \epsilon^{(c)}$
2 x 2				
4 x 4	413	376	376	371
6 x 6	413	384	384	382
8 x 8	405			

Exact value 406.

b. Clamped Edges

	$\epsilon = 0$	$\epsilon = \epsilon^{(a)}$	$\epsilon = \epsilon^{(b)}$	$\epsilon = \epsilon^{(c)}$
2 x 2	172			
4 x 4	157	123	123	120
6 x 6	135	117	117	116
8 x 8	134			

Exact value 127.

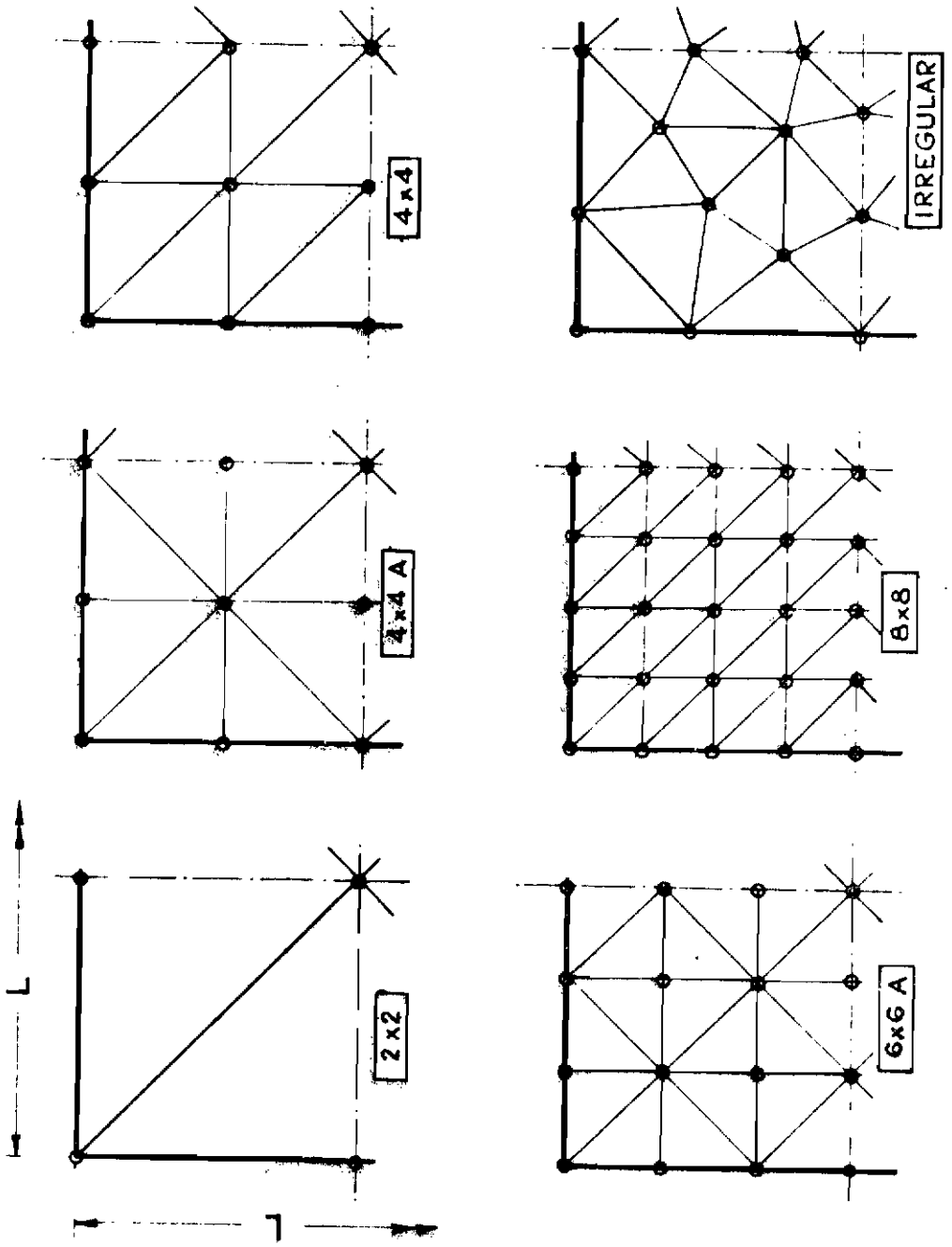

Figure 2. Square Plate - Element Divisions

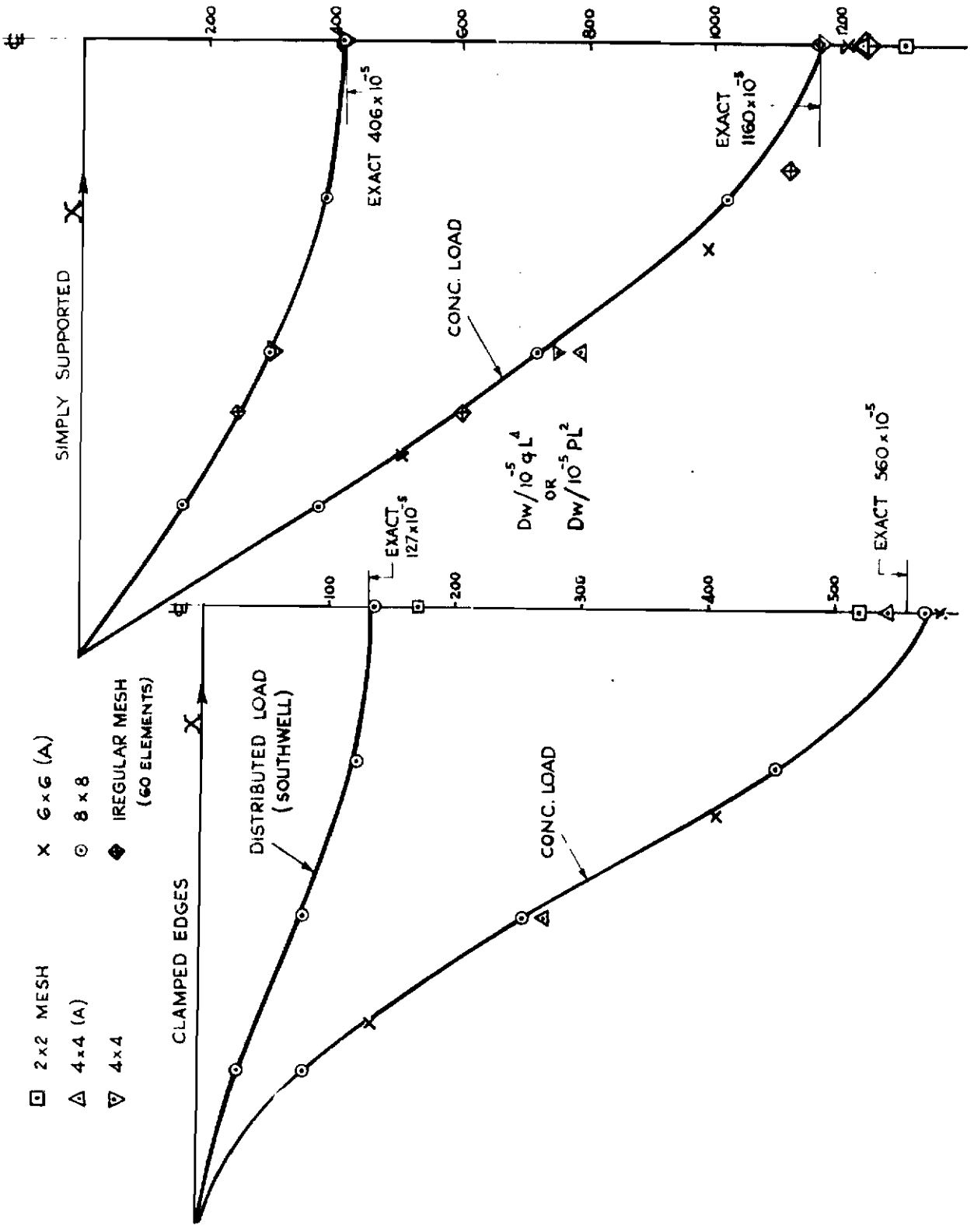

Figure 3. Square Plate Deflections on Center Line

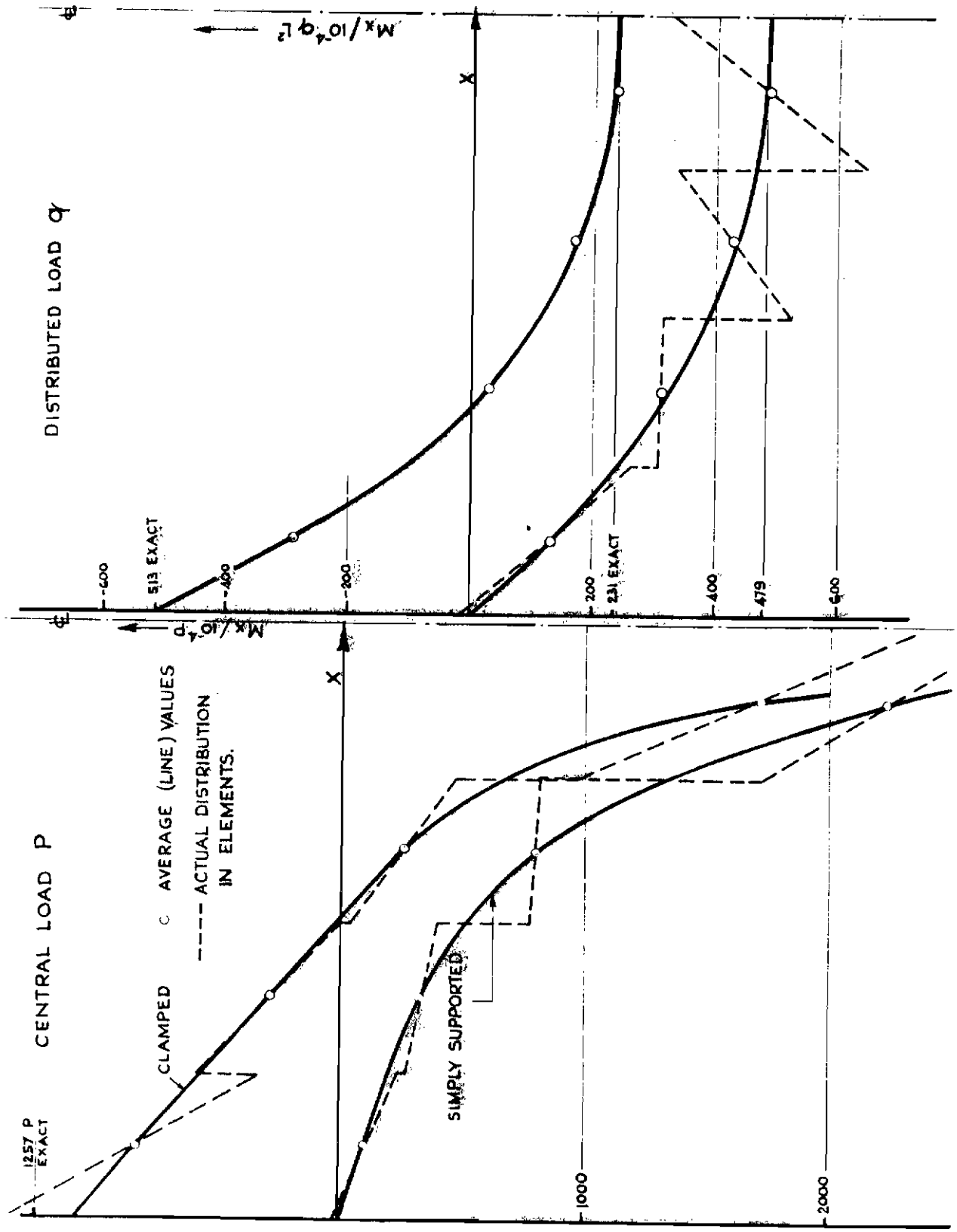

Figure 4. Square Plate Distribution of M_X on Center-Line

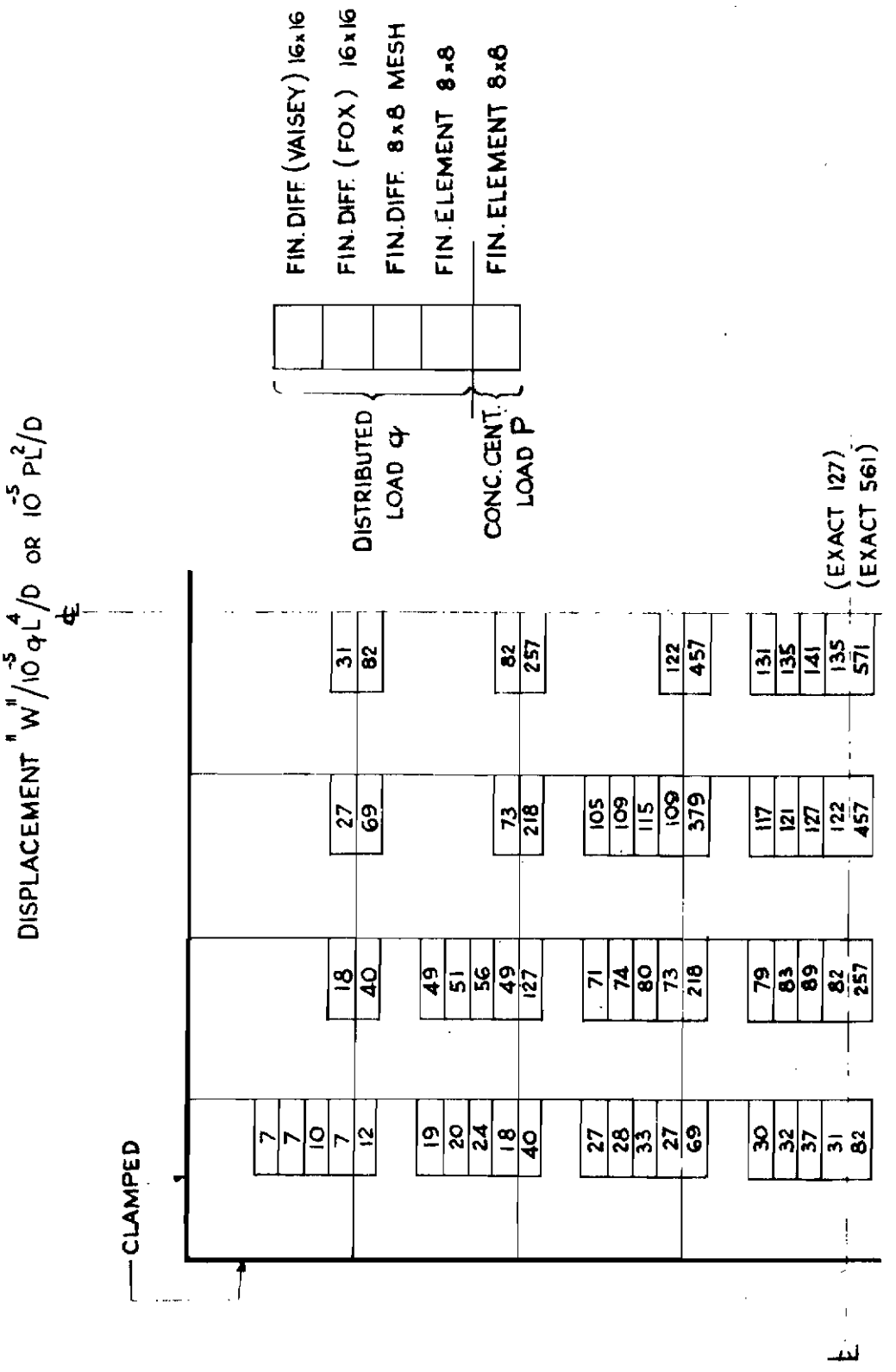

Figure 5. Square Plate. Displacement 'W' on 8x8 Mesh - Clamped Edge

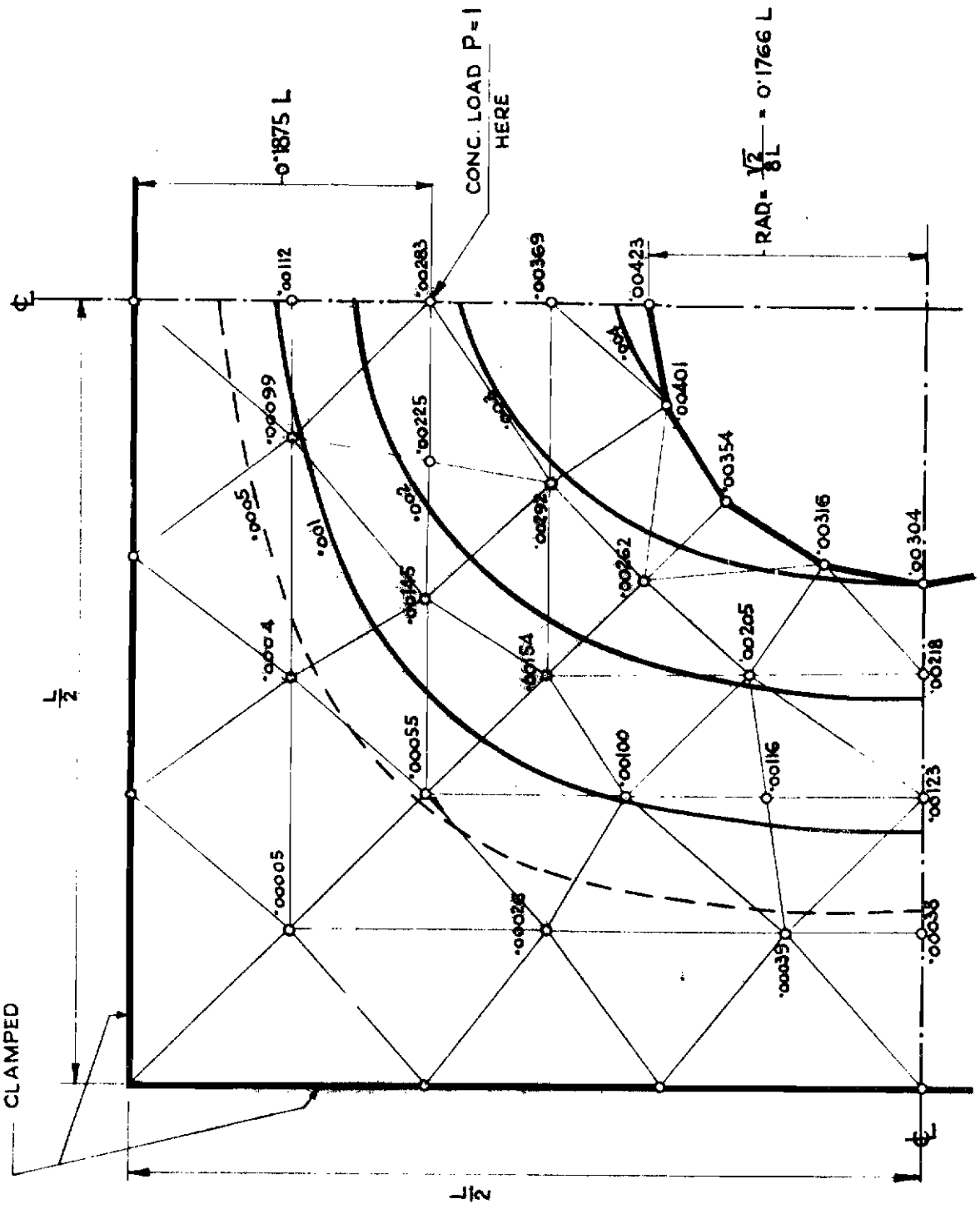

Figure 6. Square Plate with Hole. Contours-Values of Deflections (wD/PL^2)

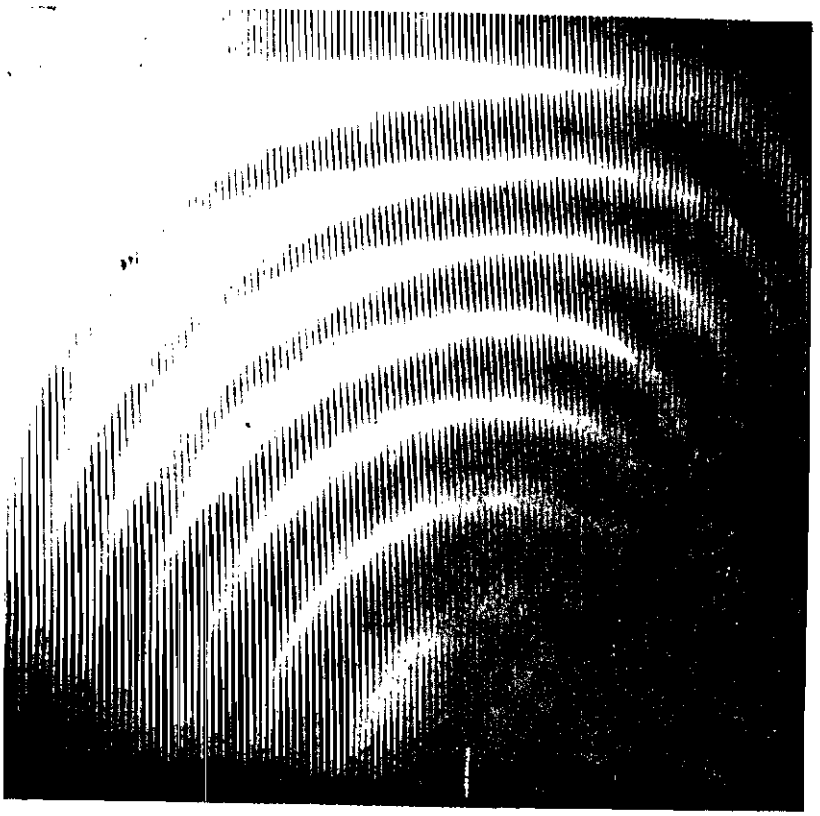

Figure 7a. As Figure 7. Slope Contours By Moire Experiment. 1 Fringe = 0.213×10^{-2}

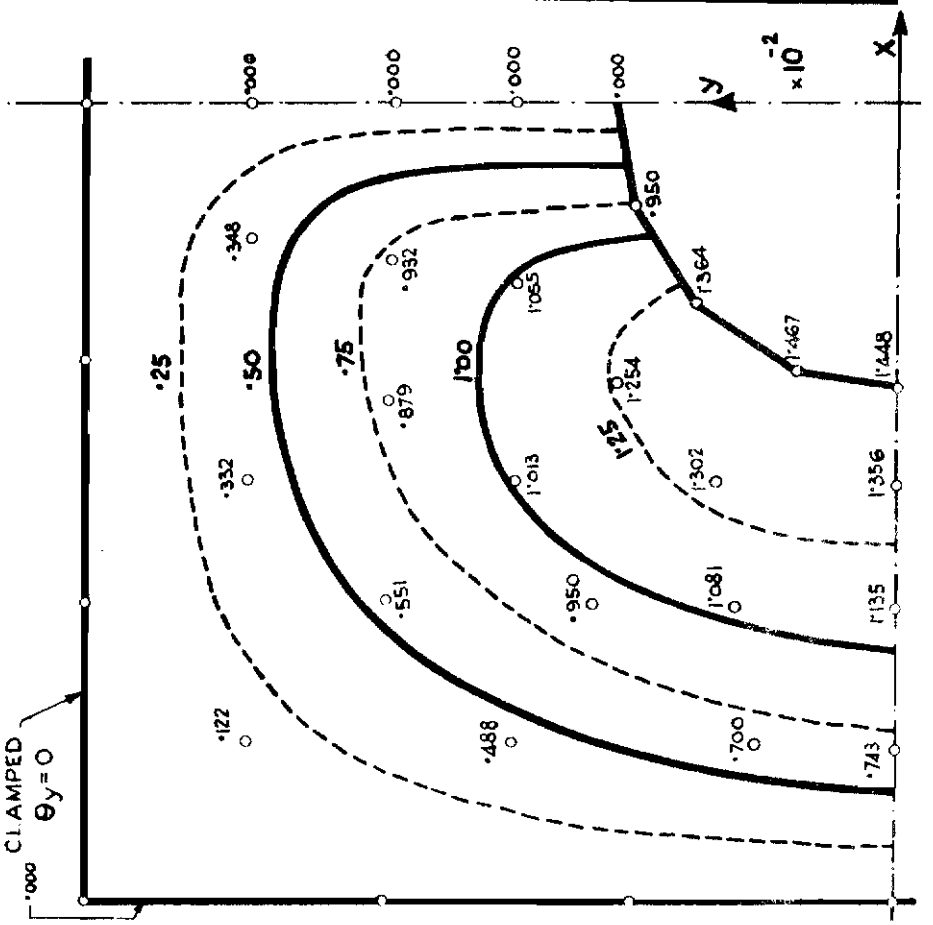

Figure 7. Square Plate with Hole. Slope Contours $\theta_y = + \frac{\partial w}{\partial x}$

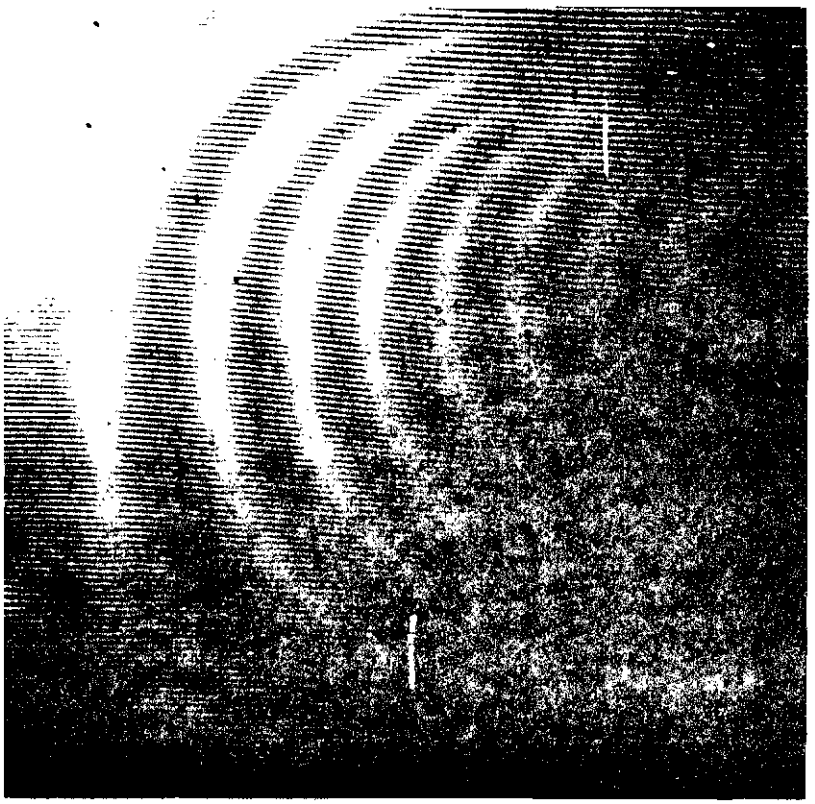

Figure 8a. As Figure 8. Slope Contours By Moire Experiment. 1 Fringe = 0.213×10^{-2}

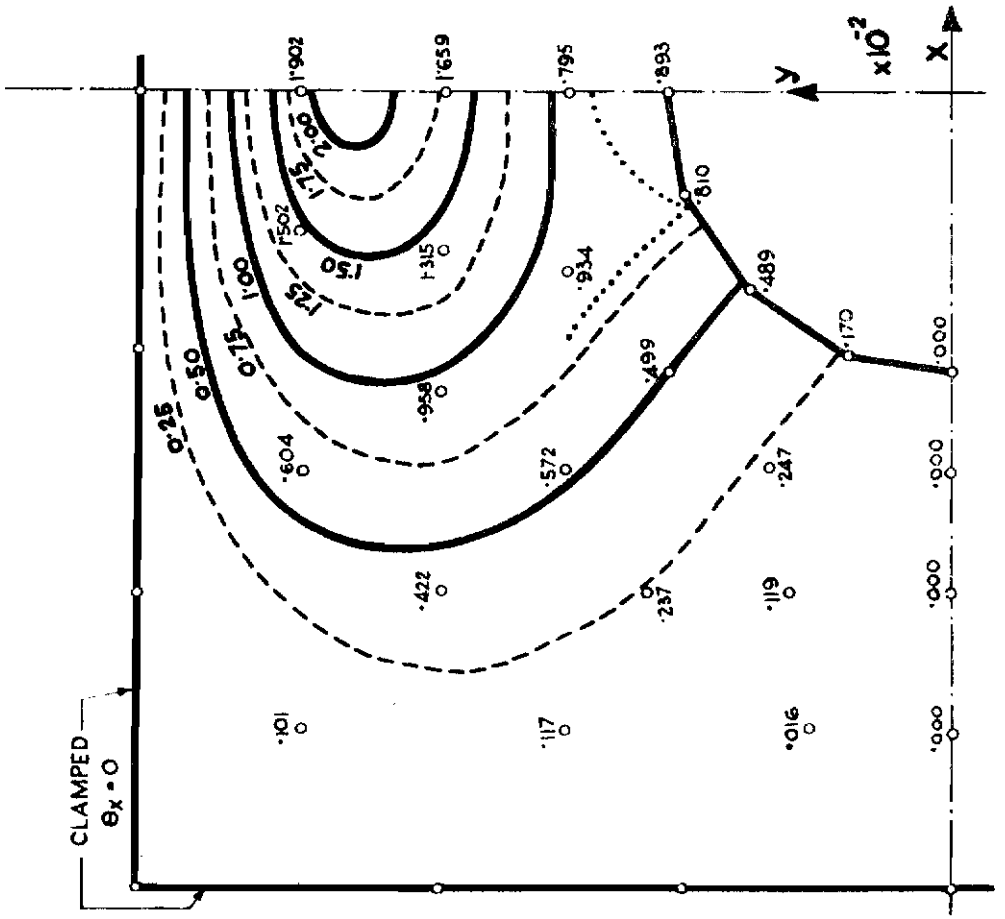

Figure 8. Square Plate with Hole. Slope Contours $\theta_x = -\frac{\partial w}{\partial y}$

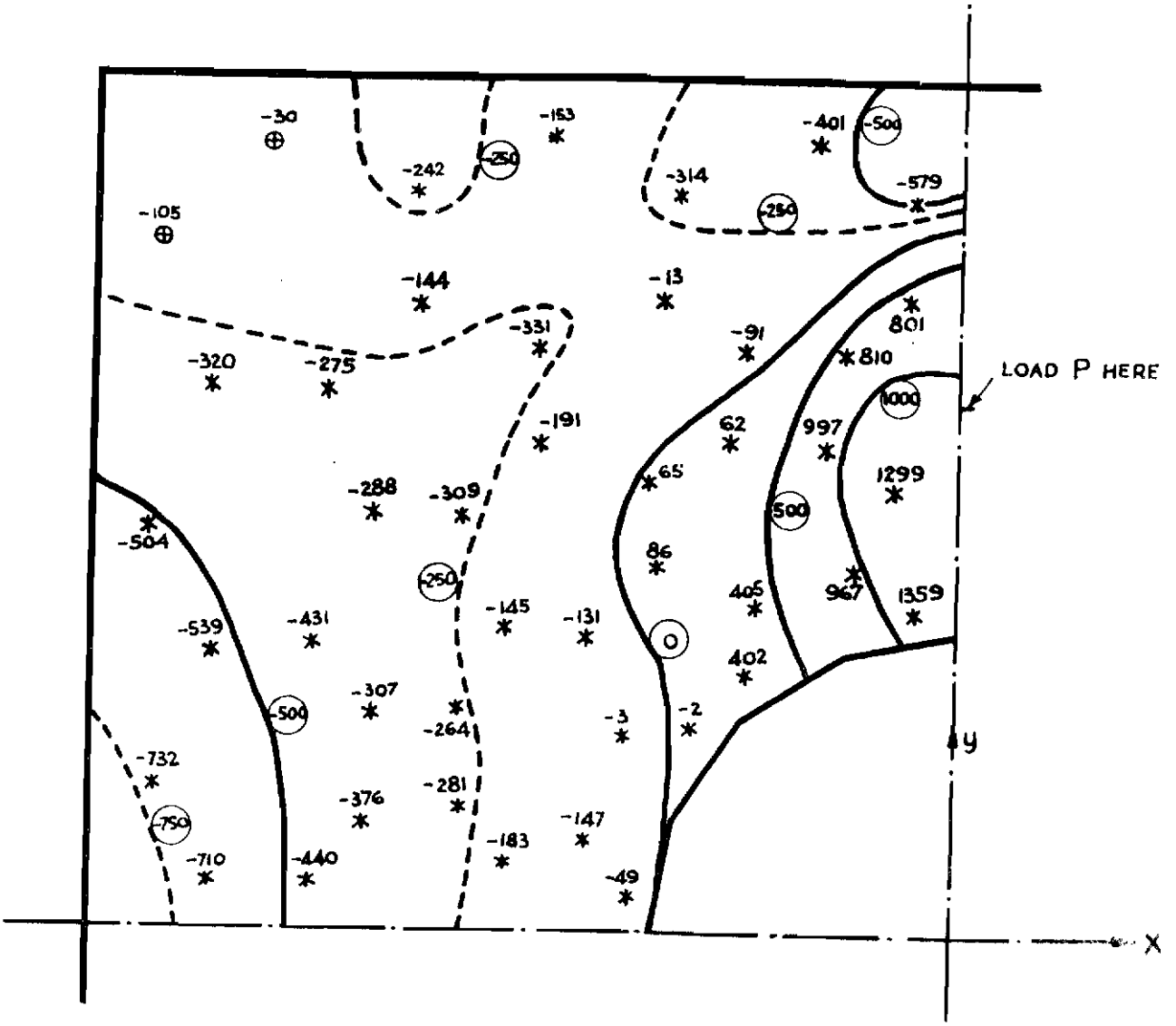

Figure 9. Square Plate with Hole. Values of M_x/P (Averaged at Centroids of Elements.)

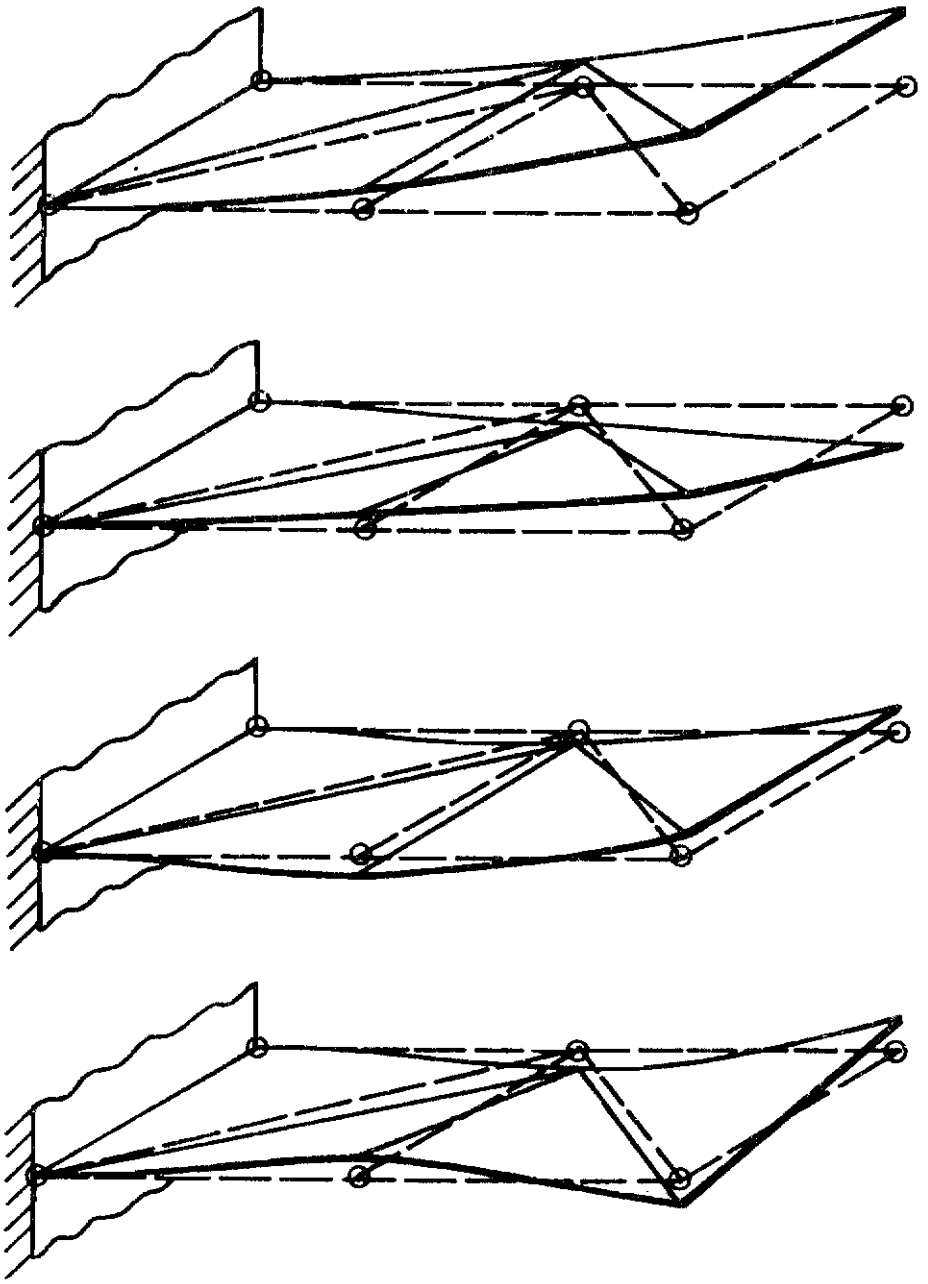

1 st. MODE.
846
826
861
962
864

2 nd. MODE.
3,638
3,728
4,293
4,300
4,369

3 rd. MODE.
5,266
5,157
6,456
6,478
6,578

4 th. MODE.
11,870
12,055
15,813
15,904
16,585

Values of frequencies are given in the following order:-

(1) Exact (ref. 17).
(2) Non conforming $\epsilon = 0$
(3) $\epsilon = \epsilon^a$
(4) $\epsilon = \epsilon^b$
(5) $\epsilon = \epsilon^c$

} Conforming

Data:-

Steel $E = 30 \times 10^6$ p.s.i.
thickness of plate = 0.1 in.
$\nu = 0.3$

Figure 10. Vibration of a Cantilever Plate Divided into Four Elements. Modal Shapes.

ADDENDUM

1. Introduction

The theoretical interest of these results centers on what happens in the limiting case, with a very fine mesh of nonconforming elements. Experiments have been done to clarify the situation: they avoided using an extensive mesh by postulating a repeating pattern, and reproducing analytically the conditions for large-scale constant curvature.

The numerical results indicate that certain mesh patterns converge correctly, whereas others do not, and theory confirms and amplifies this conclusion. Thus in Figure 10 fig. (a) converges, while (d) and (e) do not. The more general patterns (b) and (c) assure convergence for aelotropic plates, with or without conformity, provided only that the individual elements can accept constant curvature.

2. A Non-Converging Solution

The mesh of Figure 10(d) is regarded as a recurring pattern of squares containing 4, 8, or 16 triangular elements, as shaded in the diagram. Assuming that the mesh deforms on a large scale to $w = \frac{1}{2}x^2$, $\frac{1}{2}y^2$, or xy, and that the nodes are unloaded, one can apply symmetry and recurrence relations to discover the local perturbations. These falsify the effective bending flexibilities and anticlastic effects for a fine-mesh continuum, which are now summarized for $\nu = 0.3$.

$$\begin{bmatrix} w_{xx} \\ w_{yy} \\ w_{xy} \end{bmatrix} = \begin{bmatrix} 1.0177 & -.2823 & 0 \\ -.2823 & 1.0177 & 0 \\ 0 & 0 & 0.65 \end{bmatrix} \begin{bmatrix} M_x \\ M_y \\ M_{xy} \end{bmatrix}$$

instead of

$$\begin{bmatrix} 1 & -\nu & 0 \\ -\nu & 1 & 0 \\ 0 & 0 & \frac{1}{2}(1+\nu) \end{bmatrix} \begin{bmatrix} M_x \\ M_y \\ M_{xy} \end{bmatrix}$$

Evidently mesh (d) does not converge: for the typical triangle (1) the local deviations from pure bending are shown in table (j).

3. Proofs Concerning Constant Curvature Regions

We now prove that perturbations do not occur in pattern (b). Consider the minimum parallelogram mesh of (f). If the eight outer nodes are given slopes and deflections corresponding to constant curvature, it is desirable that the central node automatically takes slopes and deflection giving constant curvature in all four elements. It then follows that a larger region of elements (b) accepts any constant curvature that the boundary nodes dictate.

We therefore show that if mesh (f) is given unit curvatures w_{xx}, w_{yy} and w_{xy} in turn, the inner node 0 remains unloaded. A plate having the most general elastic properties gives the strain energy:

$$\frac{1}{2} \begin{bmatrix} w_{xx} & w_{yy} & w_{xy} \end{bmatrix} D \begin{bmatrix} w_{xx} \\ w_{yy} \\ w_{xy} \end{bmatrix} d(\text{area})$$

where D is positive definite: six independent bending moduli are implied. Due to unit curvature w_{xx} for example the force W_o is

$$\left[\frac{\partial w_{xx}}{\partial w_o} \quad \frac{\partial w_{yy}}{\partial w_o} \quad \frac{\partial w_{xy}}{\partial w_o}\right] D \begin{bmatrix} 1 \\ 0 \\ 0 \end{bmatrix} d(\text{area})$$

Therefore it is sufficient to show that the nine integrals typified by

$$(a) \iint \frac{\partial w_{xx}}{\partial w_o} d(\text{area}) \qquad (b) \iint \frac{\partial w_{xy}}{\partial (\theta_x)_o} d(\text{area})$$

integrate to zero over the four elements. Consider the sum of the contributions to (a) from equal elements of area at points A, B, C and D. The sum of the values of w_{xx} at these four points is equal to the w_{xx} in an element whose four vertices all have unit w and zero slopes. But an element that respects constant curvatures moves as a rigid body under these conditions: therefore $\Sigma w_{xx} = 0$ and the integral is zero. Similarly, (b) is zero because the values of w_{xy} due to unit (θ_x) at O are equal and opposite at symmetrically opposite points like F and G.

The availability of constant curvature regions is clearly a necessary condition for convergence: it will also be shown to be sufficient. Meanwhile, it is interesting to attempt the same proof with the mesh (d) which is known not to converge. From the minimum mesh (g) it is clearly valid to pair the contributions from K and L, so that the slope integrals like $\partial w_{xy}/\partial(\theta_x)_o$ are zero as before. Pairing contributions from K and M shows that the integral of $\partial w_{xy}/\partial w_o$ is zero. However, no such pairing is possible when integrating $\partial w_{xx}/\partial w_o$ and $\partial w_{yy}/\partial w_o$. This accords with the numerical result that isotropic mesh responds correctly to twist, $w = xy$, but not to bending.

Another non-converging mesh is illustrated in (e). Here the pairing of R and S is valid, but the pairing of R and T is not. Only the integrals of

$$\partial w_{xy}/\partial(\theta_x)_o, \quad \partial w_{xy}/\partial w_o, \quad \partial w_{xx}/\partial(\theta_y)_o, \quad \partial w_{yy}/\partial(\theta_y)_o$$

are zero, that is, only four out of the nine required. Thus convergence is most unlikely, and this case has not been investigated numerically.

4. Proof of Convergence

It is now argued that the physical problem is perturbated in various ways by a finite element solution as depicted in Figure 11(d). Consider the real plate, with a mesh of parallelograms, each of ruling dimension d, marked out over its surface. Assume that the nodal slopes and deflections are as in the real plate. (Elsewhere they are different.) The perturbations are treated under three headings:

i) Nodal forces. To deduce the order of magnitude of these, they are expressed as e.g.

$$W_o = \iint \left(M_x \frac{\partial w_{xx}}{\partial w_o} + M_y \frac{\partial w_{yy}}{\partial w_o} + 2M_{xy} \frac{\partial w_{xy}}{\partial w_o}\right) d(\text{area})$$

Two cases must be distinguished: (1) if w cannot express constant curvature, hence constant bending moments, over a region, as in meshes (d) and (e). The nodal forces W_o are of order M, and the nodal moments are of order Md. (2) if w can express constant bending moment over a region, as in meshes (a), (b) and (c). The nodal forces W_o are of order $M^1 d$, where

M' is a derivative of M, and the nodal moments are of order $M'd^2$. Because in a problem with constant bending moment (a) gives an error of a few percent, and the nodal perturbations (b) are of lower order if d is small, the error vanishes with d.

ii) Element forces. First, spurious body forces in the finite element solution may be calculated from the equations of equilibrium. Because σ = constant on the surface is available, and σ is nearly constant over the element, the body forces are of order σ'. (One can therefore argue that they are of the same order as the external body forces: in practice they are probably considerably larger.) Second, boundary tractions may be postulated. Regard the stresses at the boundaries between elements (indeterminate in a finite element solution) as taking their values in the real plate: this defines the tractions as stress-adjusters of order $\sigma' d$. Together, these element forces are in equilibrium with any external body forces over the element: we must show that they are equivalent. By St. Venant's principle, they are equivalent a few elements away. The strains in the element itself an and its immediate neighbors are of order $\epsilon' d$. Therefore the error decreases with d.

iii) Hinging between elements. To assess the effects of a small misfit, we apply it after the structure is fully loaded, and calculate the work done. Here, the strain energy per element is of order $\rho M d^2$. The hinging angle is of order $\rho' d^2$, and the work done by the misfit is of order $M\rho' d^3$. Thus the total effect of hinging is insignificant with small d: also the effect of each misfit is small compared with a typical element contribution.

5. Conclusions

It has been shown that a mesh of aelotropic parallelograms converges, because the physical perturbations introduced by the finite element become unimportant with small elements. The mesh of aelotropic triangles (c) is a special case, and it also converges. The main paper has shown that triangular meshes drawn to no particular pattern give results acceptable for engineering purposes.

Unacceptable errors could arise where large and small elements meet, or where the thickness changes. It would be an easy matter to enforce slope conformity only, for example, along a discontinuity of thickness, thus minimizing the constraints and using mostly the model known to give rapid convergence. The authors intend to use nonconforming elements exclusively, unless practical results enforce a reappraisal of such mixed methods.

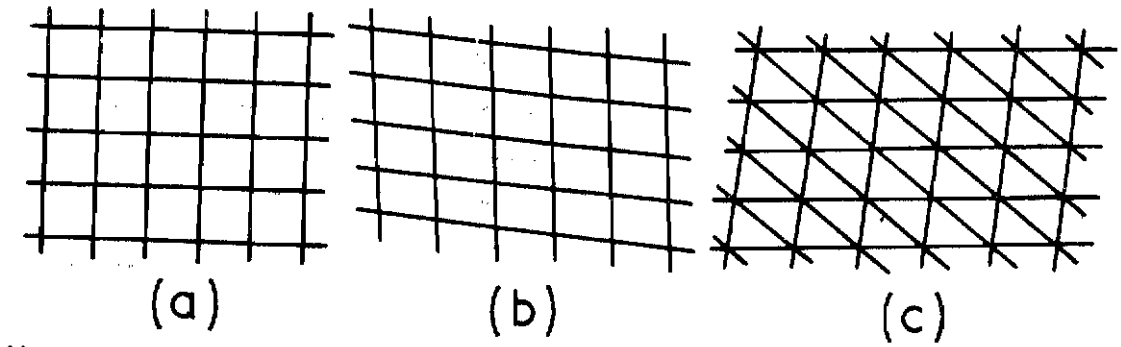

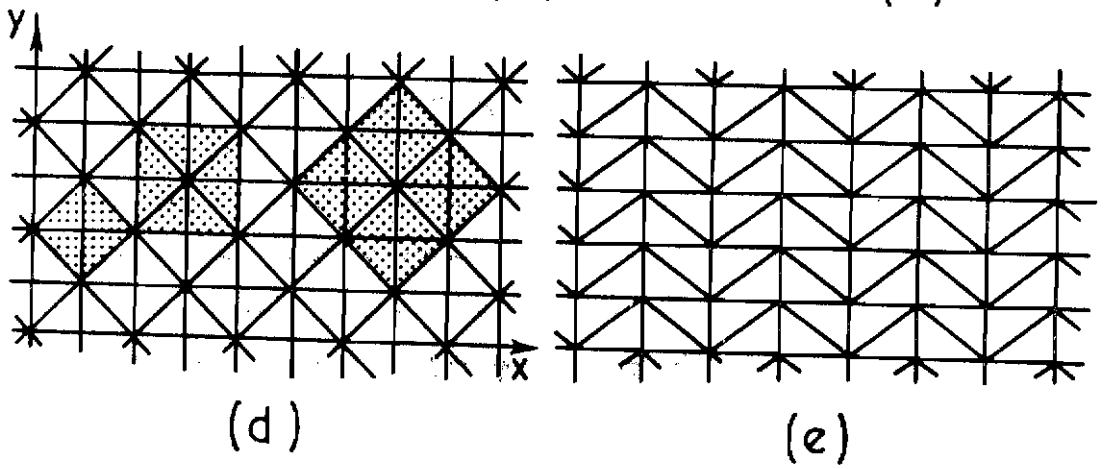

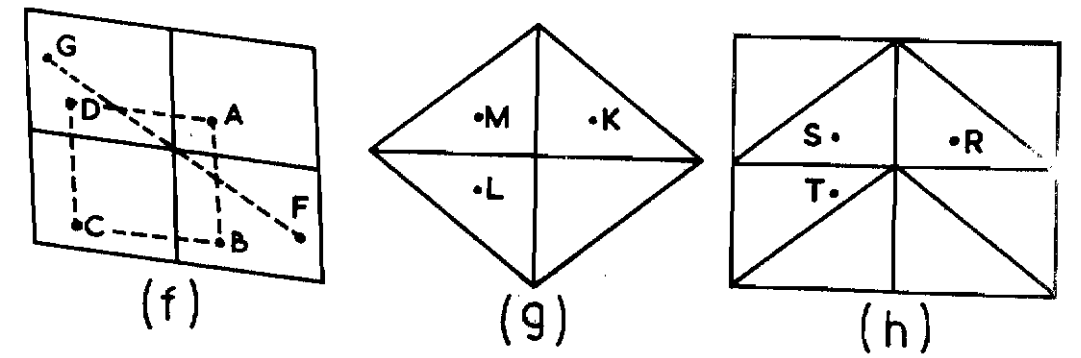

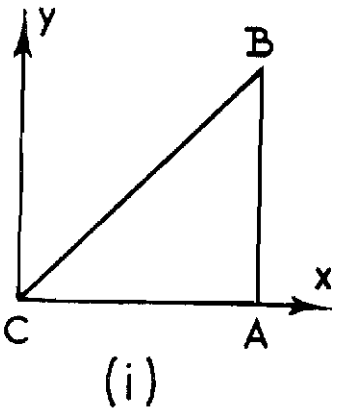

	σ_x	σ_y	τ_{xy}
A	1.252	.252	−.082
B	0.914	−.167	.082
C	0.833	−.085	.082
MEAN	1.000	.000	.027
TRUE	1	0	0

(j)

Figure 11. Diagram of Mesh Patterns